Strain-Coupling Effects in Steady Flows

J. S. VRENTAS, C. M. VRENTAS

Department of Chemical Engineering, The Pennsylvania State University, University Park, Pennsylvania 16802

Received 22 July 1996; accepted 25 October 1996

ABSTRACT: Predictions are carried out using strain-coupling theory for four steady flows: steady shear, steady planar extension, steady uniaxial extension, and steady equibiaxial extension. The general features of the steady flow predictions are compared with the general characteristics of experimental steady flow data. © 1997 John Wiley & Sons, Inc. J Appl Polym Sci **64:** 689–697, 1997

Key words: strain coupling; steady flows; nonlinear viscoelasticity

INTRODUCTION

Integral constitutive equations provide a valuable method of describing the nonlinear viscoelastic behavior of polymeric fluids. For example, one of the more useful single-integral constitutive models is the K-BKZ constitutive equation. In this constitutive theory, it is assumed that the influence of each strain increment on the stress is independent of other strain increments. To overcome some of the deficiencies of the K-BKZ theory, a somewhat more general integral model, the strain-coupling model, has been proposed.[1–4] In this constitutive theory, it is assumed that the influence of each strain increment on the stress is, in general, dependent on other strain increments, and an approximate analysis of this strain-coupling effect is developed. The objective of this article was to examine further some of the predictive capabilities of the strain-coupling theory by considering various types of steady flows.

The equations for the strain-coupling theory are presented in the second section of the article, and a modified evaluation scheme for the material functions is discussed in the third section. Some previous predictions of the strain-coupling theory in steady flows are reviewed in the fourth section, and deformation fields and viscosity ratios for the various steady flows are presented in the fifth section. Predictions of the strain-coupling model for the different types of steady flows are presented in the final section, and the general features of these predictions are compared with the general characteristics of the experimental data.

EQUATIONS FOR STRAIN-COUPLING THEORY

For the strain-coupling model, the extra stress $\boldsymbol{S}$ is described by the following equations:

$$\boldsymbol{S} = \int_0^\infty \left[\phi_1(s, I, II) + \int_0^\infty \phi_3\{s_1, s, I(s_1)\}\, ds_1 \right] [\boldsymbol{N}(s) - \boldsymbol{I}]\, ds + \int_0^\infty [\phi_2(s, I, II)][\boldsymbol{N}^{-1}(s) - \boldsymbol{I}]\, ds \quad (1)$$

$$\phi_3(s_1, s, 0) = 0 \quad (2)$$

$$I = tr[\boldsymbol{N} - \boldsymbol{I}] \quad (3)$$

$$II = \tfrac{1}{2}[I^2 - tr(\boldsymbol{N} - \boldsymbol{I})^2] = tr[\boldsymbol{N}^{-1} - \boldsymbol{I}] - 2tr[\boldsymbol{N} - \boldsymbol{I}] \quad (4)$$

Correspondence to: J. S. Vrentas.
Contract grant sponsor: Dow Chemical Co.

$$\boldsymbol{N}(s) = \boldsymbol{C}_t^{-1}(t-s) \tag{5}$$

$$\boldsymbol{N}^{-1}(s) = \boldsymbol{C}_t(t-s) \tag{6}$$

For these equations, t is the present time; s, the backward running time; $\boldsymbol{C}_t(t-s)$, the right Cauchy–Green tensor relative to time t; $\boldsymbol{I}$, the identity or unit tensor; and ϕ_1, ϕ_2, and ϕ_3, three scalar-valued material functions. The K-BKZ model is a special case of the strain-coupling theory with $\phi_3 = 0$. It is clear that the strain-coupling theory offers the possibility of better predictive capabilities for viscoelastic flows than does the K-BKZ theory because it represents a reduced version of simple fluid theory with strain-coupling effects included.[1] For the K-BKZ model, coupling of strains is assumed to be negligible.

From the above equations, it is evident that the strain-coupling model can be used to describe nonlinear rheological behavior if the material functions ϕ_1, ϕ_2, and ϕ_3 can be determined for the particular material of interest. Specific equations have been proposed[4] for the determination of these material functions for the special case of a factorable strain-coupling model. If it can be assumed that time–strain factorability is applicable for a particular material, then the shear stress for a viscoelastic fluid can be written in the following factored form for single-step shear strain stress relaxation experiments:

$$\sigma(\gamma_1, t) = \gamma_1 G(t) h(\gamma_1^2) \tag{7}$$

In this equation, γ_1 is the instantaneous shear strain applied at $t = 0$; $\sigma(\gamma_1, t)$, the shear stress for $t > 0$; $G(t)$, the shear stress relaxation modulus of linear viscoelasticity; and $h(\gamma_1^2)$, a monotonically decreasing function of strain with $h(0) = 1$. For some materials, the factored form given by eq. (7) is valid for a wide range of γ_1, and, for many materials, time–strain factorability is valid at least for sufficiently low values of γ_1. For the factorable strain-coupling model, the following equations have been proposed for the material functions ϕ_1, ϕ_2, and ϕ_3[4]:

$$\phi_1(s, I, II) = \frac{m(s) H^*(I^*)}{1+\epsilon} \tag{8}$$

$$\phi_2(s, I, II) = -\frac{m(s)\epsilon H^*(I^*)}{1+\epsilon} \tag{9}$$

$$m(s) = -\frac{dG(s)}{ds} \tag{10}$$

$$\phi_3\{s_1, s, I(s_1)\} = \beta(s_1, s) K[I(s_1)] \tag{11}$$

$$h(I) = H^*(I) + K(I) \tag{12}$$

$$\beta(s, s_1) = \frac{9}{1-k} \sum_{i=1}^{N} \frac{a_i}{\lambda_i} e^{8s/\lambda_i} e^{-9s_1/\lambda_i} \quad s_1 > s \tag{13}$$

$$\beta(s, s_1) = -\frac{9k}{1-k} \sum_{i=1}^{N} \frac{a_i}{\lambda_i} e^{-9s/\lambda_i} e^{8s_1/\lambda_i} \quad s > s_1 \tag{14}$$

$$\frac{K(I)}{8(1-k)} = \frac{h(4I) - h(I)}{2} \tag{15}$$

$$I^* = \frac{I(1+2\epsilon)}{1+\epsilon} + \frac{\epsilon II}{1+\epsilon} \tag{16}$$

In these equations, k and ϵ are constants and a_i and λ_i are constants in the usual expression for $m(t)$:

$$m(t) = \sum_{i=1}^{N} a_i e^{-t/\lambda_i} \tag{17}$$

The constant ϵ can be evaluated from steady shear data using the expression

$$\left[-\frac{N_2(\dot{\gamma})}{N_1(\dot{\gamma})}\right]_{\dot{\gamma}=0} = \frac{\epsilon}{1+\epsilon} \tag{18}$$

where N_1 and N_2 are the first and second normal stress differences and $\dot{\gamma}$ is the shear rate for the steady shear flow. In addition, the constant k can be calculated from the following expressions which are valid for low to moderate strain levels:

$$k = \frac{2}{3} \frac{[-1-\xi]}{[1-\xi]} \tag{19}$$

$$\xi = \frac{\dfrac{K(9\gamma^2)}{8(1-k)}}{\dfrac{K(\gamma^2)}{8(1-k)}} \tag{20}$$

where γ is the applied shear strain in a step strain experiment. The calculation of k can be made somewhat more explicit by noting that the quantity $K/8(1-k)$ [which is calculated from eq. (15)] can generally be written in the following form for low values of the strain γ:

$$-\frac{K(\gamma^2)}{8(1-k)} = C(\gamma^2)^p \tag{21}$$

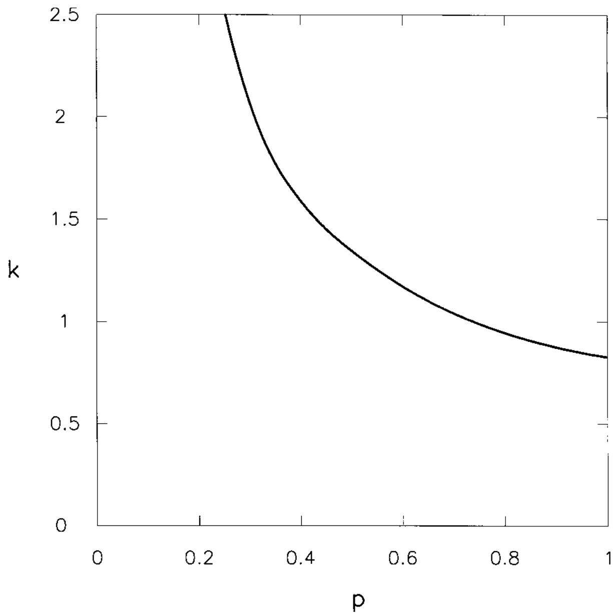

Figure 1 Graphical representation of dependence of k on exponent p as described by eq. (22).

Here, C is a constant and $p > 0$. Consequently, eq. (19) can now be written as follows:

$$k = \frac{2}{3}\left[\frac{-1 - 9^p}{1 - 9^p}\right] \tag{22}$$

so that k can be simply evaluated once p is determined. The dependence of k on the exponent p is illustrated in Figure 1. The new procedure for directly calculating k from eq. (22) (essentially using only single-step data) gives values of k which are comparable to those calculated using double-step shear strain stress relaxation experiments.[4] For example, for an IUPAC branched low-density polyethylene sample, a value of $k = 1.51$ is calculated using double-step data and a value of $k = 1.62$ is computed using eq. (22). For a polystyrene–dibutyl phthalate solution, double-step data yield a value of $k = 0.86$ and a value of $k = 0.90$ is calculated from eq. (22). Consequently, it appears that good estimates of k can be derived without using double-step experiments. The above set of equations can be used to determine the material functions ϕ_1, ϕ_2, and ϕ_3, and the evaluation scheme for these material functions is summarized in the next section.

EVALUATION OF MATERIAL FUNCTIONS

The material functions of the strain-coupling theory can be evaluated using single-step shear strain stress relaxation experiments and a small amount of data from steady shear experiments. For materials for which time–strain factorability is applicable, the following procedure can be used to determine the material functions, ϕ_1, ϕ_2, and ϕ_3 of the strain-coupling theory:

1. A series of single-step shear strain stress relaxation experiments is carried out on the material of interest over an appropriate range of γ_1, the applied shear strain. The shear stress vs. time data from such experiments can be used with eq. (7) to determine $G(t)$ (from the linear part of the data) and $h(I)$ (from the nonlinear part of the data). The $G(t)$ data can be used in eq. (10) to yield $m(t)$, and the parameters a_i and λ_i can be determined from eq. (17) using standard procedures.
2. The $h(I)$ data can be used in eq. (15) to determine the function $K(I)/(1 - k)$ over an appropriate range of I.
3. The $K(I)/(1 - k)$ results at low strains can be used with eq. (21) to determine the exponent p. A value of the parameter k for the system of interest can then be calculated using eq. (22).
4. The results of steps 2 and 3 are combined to determine $K(I)$ over the complete range of I for which $K(I)/(1 - k)$ values are available.
5. Results for a_i, λ_i, and k can be used in eqs. (13) and (14) to calculate $\beta(s, s_1)$, and ϕ_3 can then be computed from the known $K(I)$ and $\beta(s, s_1)$ from eq. (11).
6. Results for $K(I)$ and $h(I)$ can be used in eq. (12) to calculate $H^*(I)$ and, thus, $H^*(I^*)$.
7. The ratio N_2/N_1 near $\dot{\gamma} = 0$ can be measured using steady shear experiments at small shear rates. Data taken on cone-and-plate viscometers and on parallel-plate viscometers can be used to determine the ratio N_2/N_1, and the constant ϵ can be calculated from eq. (18) using the limiting value of N_2/N_1 at zero shear rate.
8. The material functions ϕ_1 and ϕ_2 can be calculated using eqs. (8) and (9) with I^* defined by eq. (16).

The present version of the strain-coupling theory is, of course, not a predictive theory since single-step stress relaxation data and a small amount of steady shear data are needed to carry out the determination of the material functions. However, such data are not particularly difficult to obtain for a given material. Furthermore, evaluation of the material functions for the strain-coupling theory requires no more data than are needed for evaluation of the material functions for the K-BKZ theory.

PREVIOUS STEADY FLOW PREDICTIONS

The strain-coupling constitutive equation has been previously used to analyze various aspects of the following experiments: double-step shear strain stress relaxation experiments[1–3,5]; start-up and cessation flow experiments[6,7]; finite amplitude oscillatory experiments[8]; extensional flow step strain experiments[4]; and steady shear and steady planar extension experiments.[9] To put the predictions presented in this study in proper context, it appears useful to summarize previous predictive results of strain-coupling theory for steady flows.

In a previous investigation of strain-coupling theory,[9] it was found that it is necessary to place some restrictions on the memory of the fluid to avoid unbounded integrals for exponential histories and to exclude the possibility of having negative viscosities for steady shear flows. The memory of the fluid can be limited by limiting the range of integration for the material, and, as is illustrated below, the finite memory of the fluid can be determined directly from previously determined rheological properties of the fluid. The approach used in the strain-coupling theory for truncating integrals cannot be used for the K-BKZ model unless additional assumptions are introduced. The fact that the strain-coupling model suggests a reasonable way to limit the memory of the fluid provides flexibility in the type of $h(I)$ functions which can be used with the model. For example, consider the following two expressions for $h(I)$ with constant parameters α or δ:

$$h(I) = \frac{1}{1 + \alpha I^{1/2}} \tag{23}$$

$$h(I) = \frac{1}{1 + \delta I} \tag{24}$$

Utilization of eq. (23) enhances the possibility of strain hardening in steady elongational flows and reduces the level of the shear thinning in steady shear flows. This equation can be used for strain-coupling theory but not for the K-BKZ theory because it yields unbounded stresses in steady elongational flows. The $h(I)$ function given by eq. (24) can be used with the K-BKZ theory, but it produces a pronounced maximum in the shear stress–shear rate curve and, in general, insufficient strain hardening. Consequently, the finite memory of the strain-coupling model allows a greater choice for $h(I)$ and, hence, the possibility of increasing the strain hardening and reducing the shear thinning. The general approach used previously will be applied below in the examination of four steady flows: steady shear, steady planar extension, steady uniaxial extension, and steady equibiaxial extension. The steady shear viscosity and the first steady planar extensional viscosity were considered in the previous study.[9] In this study, we consider predictions for the second steady planar extensional viscosity, for the steady uniaxial extensional viscosity, and for the steady equibiaxial extensional viscosity.

In the next section, deformation fields and viscosity ratios are presented for the four steady flows considered here. The four flows and five viscosity ratios are summarized in Table I. In this table, the zero subscript refers to a zero deformation rate. Laun and Schuch[10] presented shear and elongational flow data for a polyisobutylene sample and for a low-density polyethylene IUPAC X sample. They presented data for normalized versions of the five viscosities listed above. From the transient viscosity data taken at similar deformation rates, it seems reasonable to surmise that the steady-state viscosity ratios should be ordered as follows for polyethylene under comparable deformation conditions:

$$\frac{\eta_U}{\eta_{U0}} > \left(\frac{\eta_E}{\eta_{E0}}\right)_1 > \frac{\eta_B}{\eta_{B0}} > \frac{\eta}{\eta_0} > \left(\frac{\eta_E}{\eta_{E0}}\right)_2 \tag{25}$$

The position of η_B/η_{B0} is inferred from the polyisobutylene data. For the polyisobutylene system, it is possible to infer the same pattern from the transient viscosity data with the exception that $(\eta_E/\eta_{E0})_2$ is slightly greater than η/η_0. The major objective of this article was to see if the strain-coupling theory can predict the ordering presented in eq. (25) for the five viscosities for a low-density polyethylene sample subjected to the four deformation histories described above. It is necessary to emphasize that the ordering presented in eq. (25) for steady flows has been surmised from data on transient flows.

Table I Summary of Viscosity Ratios

Flow	Viscosity Ratio	Symbol
Steady shear	Steady shear viscosity ratio	$\frac{\eta}{\eta_0}$
Steady planar extension	First steady planar extensional viscosity ratio	$\left(\frac{\eta_E}{\eta_{E0}}\right)_1$
Steady planar extension	Second steady planar extensional viscosity ratio	$\left(\frac{\eta_E}{\eta_{E0}}\right)_2$
Steady uniaxial extension	Steady uniaxial extensional viscosity ratio	$\frac{\eta_U}{\eta_{U0}}$
Steady equibiaxial extension	Steady equibiaxial extensional viscosity ratio	$\frac{\eta_B}{\eta_{B0}}$

DEFORMATION HISTORIES AND VISCOSITY RATIOS

In this section, we present the deformation fields for the four steady flows under consideration and the viscosity ratios for the five steady viscosities of interest here. In all cases, a single relaxation time λ will be used in the calculation of the material functions. Also, the following dimensionless forms of the backward running times are utilized in the expressions for the viscosity ratios:

$$x' = \frac{s_1}{\lambda} \qquad (26)$$

$$x = \frac{s}{\lambda} \qquad (27)$$

The following equations describe the deformation field for a steady shear flow with a shear rate $\dot{\gamma}$:

$$[\boldsymbol{N}(s) - \boldsymbol{I}] = \begin{bmatrix} \dot{\gamma}^2 s^2 & \dot{\gamma} s & 0 \\ \dot{\gamma} s & 0 & 0 \\ 0 & 0 & 0 \end{bmatrix} \qquad (28)$$

$$[\boldsymbol{N}^{-1}(s) - \boldsymbol{I}] = \begin{bmatrix} 0 & -\dot{\gamma} s & 0 \\ -\dot{\gamma} s & \dot{\gamma}^2 s^2 & 0 \\ 0 & 0 & 0 \end{bmatrix} \qquad (29)$$

$$I = -II = \dot{\gamma}^2 s^2 \qquad (30)$$

In addition, the viscosity ratio can be expressed as follows:

$$\frac{\eta}{\eta_0} = \int_0^\infty x e^{-x} F_1(x)\, dx \qquad (31)$$

where $F_1(x)$ is defined by the following expression:

$$F_1(x) = h(z^2x^2) - \left[\frac{K(z^2x^2)}{1-k}\right](1-k) + \int_0^x \frac{9K[(zx')^2]}{1-k} \exp[-8(x-x')]\, dx' - \int_x^\infty \frac{9kK[(zx')^2]}{1-k} \exp[-9(x'-x)]\, dx' \qquad (32)$$

$$z = \dot{\gamma}\lambda \qquad (33)$$

The deformation dependence of $F_1(x)$ is obviously suppressed in eq. (31).

The following equations describe the deformation field for steady planar extension with elongation rate $\dot{\epsilon}$:

$$[\boldsymbol{N}(s) - \boldsymbol{I}] = \begin{bmatrix} e^{2\dot{\epsilon}s} - 1 & 0 & 0 \\ 0 & e^{-2\dot{\epsilon}s} - 1 & 0 \\ 0 & 0 & 0 \end{bmatrix} \qquad (34)$$

$$[\boldsymbol{N}^{-1}(s) - \boldsymbol{I}] = \begin{bmatrix} e^{-2\dot{\epsilon}s} - 1 & 0 & 0 \\ 0 & e^{2\dot{\epsilon}s} - 1 & 0 \\ 0 & 0 & 0 \end{bmatrix} \qquad (35)$$

$$I = -II = e^{2\dot{\epsilon}s} + e^{-2\dot{\epsilon}s} - 2 \qquad (36)$$

The two viscosity ratios can be expressed as follows:

$$\left(\frac{\eta_E}{\eta_{E0}}\right)_1 = \int_0^\infty e^{-x} F_2(x) \frac{\sinh 2yx}{2y}\, dx \quad (37)$$

$$\left(\frac{\eta_E}{\eta_{E0}}\right)_2 = \int_0^\infty e^{-x} F_3(x) \frac{[1 - e^{-2yx}]}{2y}\, dx + \frac{\epsilon}{1+\epsilon} \int_0^\infty e^{-x}\left[h(q_x) - \left\{\frac{K(q_x)}{1-k}\right\}(1-k)\right] \frac{[e^{2yx} - 1]}{2y}\, dx \quad (38)$$

$$q_x = e^{2yx} + e^{-2yx} - 2 \quad (39)$$

$$F_2(x) = h(q_x) - \left[\frac{K(q_x)}{1-k}\right](1-k) + \int_0^x \frac{9K(q_{x'})}{1-k} \exp[-8(x - x')]\, dx' - \int_x^\infty \frac{9kK(q_{x'})}{1-k} \exp[-9(x' - x)]\, dx' \quad (40)$$

$$F_3(x) = F_2(x) - \frac{\epsilon h(q_x)}{1+\epsilon} + \frac{\epsilon}{1+\epsilon}\left[\frac{K(q_x)}{1-k}\right](1-k) \quad (41)$$

$$y = \dot{\epsilon}\lambda \quad (42)$$

For steady uniaxial extension with elongation rate $\dot{\epsilon}$, the deformation field is described by the following equations:

$$[\boldsymbol{N}(s) - \boldsymbol{I}] = \begin{bmatrix} e^{2\dot{\epsilon}s} - 1 & 0 & 0 \\ 0 & e^{-\dot{\epsilon}s} - 1 & 0 \\ 0 & 0 & e^{-\dot{\epsilon}s} - 1 \end{bmatrix} \quad (43)$$

$$[\boldsymbol{N}^{-1}(s) - \boldsymbol{I}] = \begin{bmatrix} e^{-2\dot{\epsilon}s} - 1 & 0 & 0 \\ 0 & e^{\dot{\epsilon}s} - 1 & 0 \\ 0 & 0 & e^{\dot{\epsilon}s} - 1 \end{bmatrix} \quad (44)$$

$$I = e^{2\dot{\epsilon}s} + 2e^{-\dot{\epsilon}s} - 3 \quad (45)$$

$$II = e^{-2\dot{\epsilon}s} - 2e^{2\dot{\epsilon}s} + 2e^{\dot{\epsilon}s} - 4e^{-\dot{\epsilon}s} + 3 \quad (46)$$

The viscosity ratio is given by the expression

$$\frac{\eta_U}{\eta_{U0}} = \int_0^\infty e^{-x} F_4(x) \frac{[e^{2yx} - e^{-yx}]}{3y}\, dx - \frac{\epsilon}{1+\epsilon} \int_0^\infty e^{-x}\left[h(I^*) - \left\{\frac{K(I^*)}{1-k}\right\}(1-k)\right] \times \frac{[e^{-2yx} - e^{yx}]}{3y}\, dx \quad (47)$$

where

$$F_4(x) = \frac{h(I^*)}{1+\epsilon} - \left[\frac{K(I^*)}{1-k}\right]\frac{(1-k)}{1+\epsilon} + \int_0^x \frac{9K[I(x')]}{1-k} \exp[-8(x - x')]\, dx' - \int_x^\infty \frac{9kK[I(x')]}{1-k} \exp[-9(x' - x)]\, dx' \quad (48)$$

$$I(x) = e^{2yx} + 2e^{-yx} - 3 \quad (49)$$

$$II(x) = e^{-2yx} - 2e^{2yx} + 2e^{yx} - 4e^{-yx} + 3 \quad (50)$$

$$I^* = \frac{1+2\epsilon}{1+\epsilon} I(x) + \frac{\epsilon}{1+\epsilon} II(x) \quad (51)$$

For steady equibiaxial extension with elongation rate $\dot{\zeta}$, it is clearly possible to consider the equibiaxial extension as a special type of a uniaxial experiment with a compression in the stretching direction. Hence, the steady equibiaxial extensional flow is described by eqs. (43)–(51) with a value of $\dot{\epsilon} = -2\dot{\zeta}$. It is thus possible to compute equibiaxial results from the uniaxial equations by using a negative value of $\dot{\epsilon}$. The deformation rates and dimensionless deformation rates for the four flows are summarized in Table II.

The five viscosity ratios can thus be calculated using eqs. (31), (37), (38), and (47) with the infinite integrals in these equations being terminated at a finite value of x. The upper limits in these integrals are determined using the characteristics of $F_1(x)$, $F_2(x)$, $F_3(x)$, and $F_4(x)$. Each of these functions is positive at $x = 0$ and each goes to zero at some finite value of x. Since these four functions are essentially weighting functions for the strains in the material, it is reasonable to suppose that strains for larger values of x do not contribute to the stress. Such strains are effectively eliminated from the stress calculation by using finite values of x for the upper limits in the integrals in eqs. (31), (37), (38), and (47). In general, the $F_I(x)$ functions are coefficients for the

Table II Summary of Deformation Rates

Flow	Deformation Rate	Dimensionless Deformation Rate	Independent Variables for Viscosity Ratio
Steady shear	$\dot{\gamma}$	$z = \dot{\gamma}\lambda$	$k, \alpha z$
Steady planar extension (first viscosity)	$\dot{\epsilon}$	$y = \dot{\epsilon}\lambda$	k, y, α
Steady planar extension (second viscosity)	$\dot{\epsilon}$	$y = \dot{\epsilon}\lambda$	k, ϵ, y, α
Steady uniaxial extension	$\dot{\epsilon}$	$y = \dot{\epsilon}\lambda$	k, ϵ, y, α
Steady equibiaxial extension	$\dot{\zeta}$	$w = \dot{\zeta}\lambda$	k, ϵ, w, α

strains computed using $[\boldsymbol{N}(s) - \boldsymbol{I}]$ in eq. (1). This is the case for $F_3(x)$ and $F_4(x)$. However, in some cases (steady shear and the first viscosity for steady planar extension), the components of $\boldsymbol{N}(s) - \boldsymbol{I}$ and $\boldsymbol{N}^{-1}(s) - \boldsymbol{I}$ have the same magnitude, and, hence, the coefficient of $\boldsymbol{N}^{-1}(s) - \boldsymbol{I}$ is included in $F_1(x)$ and $F_2(x)$. A separate truncation procedure is applied for each strain component, although the upper limit in the integral will be the same for all strains if only the coefficient of $\boldsymbol{N}(s) - \boldsymbol{I}$ is included in the $F_I(x)$. The truncation method is applied here only for steady flows. A similar approach must be used for transient deformations as they approach the steady-state limit. An example of the x and deformation dependence of $F_2(x)$ is presented elsewhere.[9]

RESULTS AND DISCUSSION

Predictions for the five viscosity ratios considered in this study are presented below with $h(I)$ calculated using eq. (23). For this choice for $h(I)$, the five viscosity ratios depend on two, three, or four variables. The variable dependence of each of the viscosity ratios is summarized in Table II. For this study, predictions were carried out for one value of ϵ (0.25), for two values of k ($\frac{7}{8}$ and 1.5), and for two values of α(0.1 and 0.2). A value of $\epsilon = 0.25$ is close to the ϵ value calculated for a low-density polyethylene sample.[4] In addition, a value of $k = 1.5$ represents a branched low-density polyethylene sample, and a value of $k = \frac{7}{8}$ represents a linear polystyrene solution.[3]

Predictions for the dependence of the viscosity ratio on the dimensionless deformation rate are presented in Figure 2 (for $\epsilon = 0.25$, $k = 1.5$, and $\alpha = 0.1$), in Figure 3 (for $\epsilon = 0.25$, $k = 1.5$, and $\alpha = 0.2$), and in Figure 4 (for $\epsilon = 0.25$, $k = \frac{7}{8}$, and $\alpha = 0.1$). The predictions in Figures 2 and 3 should be generally applicable to a low-density polyethylene sample. Three of the viscosities in

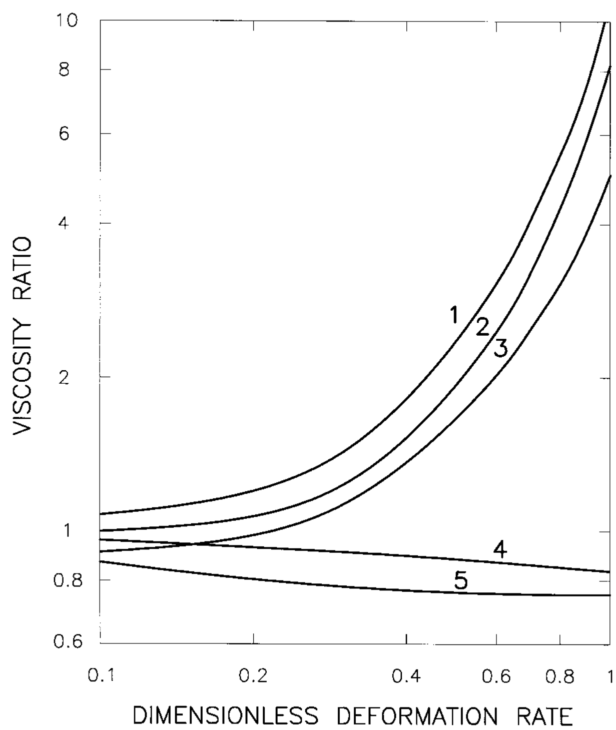

Figure 2 Dependence of viscosity ratio on dimensionless deformation rate for $\epsilon = 0.25$, $k = 1.5$, and $\alpha = 0.1$. Curve 1, uniaxial extensional viscosity ratio; curve 2, first planar extensional viscosity ratio; curve 3, equibiaxial extensional viscosity ratio; curve 4, shear viscosity ratio; curve 5, second planar extensional viscosity ratio.

these two figures exhibit significant strain hardening (an increase in viscosity with increasing deformation rate) and two essentially exhibit only shear thinning (a decrease in viscosity with increasing deformation rate). In addition, the ordering of the steady viscosity ratios in these two figures for sufficiently high deformation rates is exactly the same as that surmised above from transient experiments [eq. (25)]. Hence, the general features of the predictions of the strain-coupling model for a low-density polythylene-type system (with $\epsilon = 0.25$ and $k = 1.5$) are in good agreement with general characteristics surmised from experimental data for a low-density polyethylene sample. It is further evident from Figures 2 and 3 that the effect of increasing α, with ϵ and k fixed, is to decrease the level of strain hardening and to increase the level of shear thinning.

Comparison of Figure 4 with Figures 2 and 3 indicates that the results for $k = \frac{7}{8}$ differ in two ways from those for $k = 1.5$. First, four of the viscosities for $k = \frac{7}{8}$ exhibit significant strain hardening as compared with three for $k = 1.5$. Only

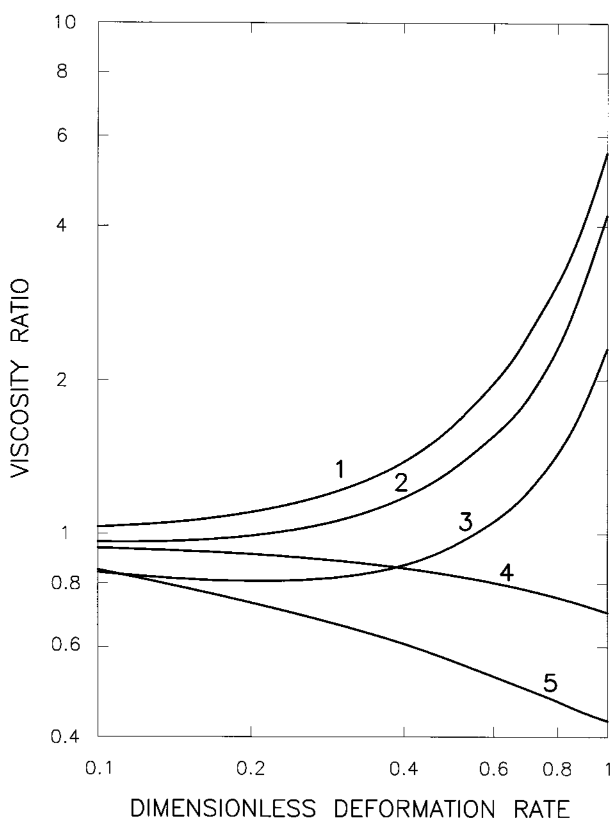

Figure 3 Dependence of viscosity ratio on dimensionless deformation rate for $\epsilon = 0.25$, $k = 1.5$, and $\alpha = 0.2$. Curves are defined as in Figure 2.

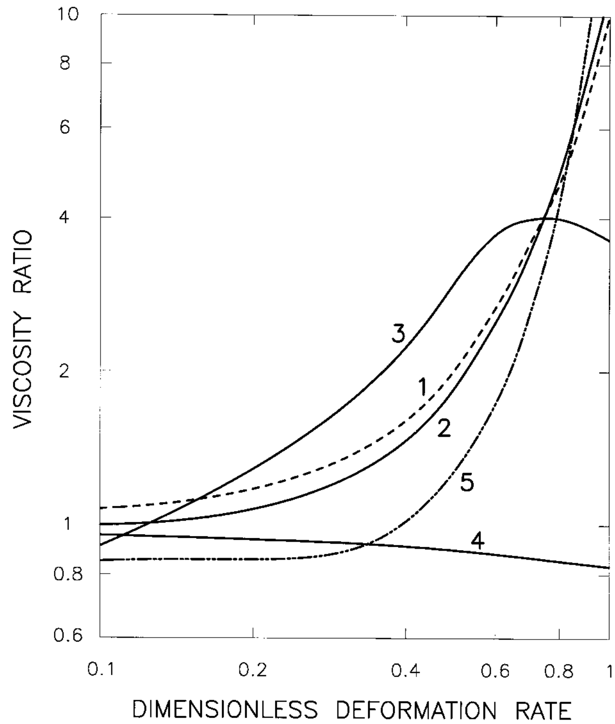

Figure 4 Dependence of viscosity ratio on dimensionless deformation rate for $\epsilon = 0.25$, $k = \frac{7}{8}$, and $\alpha = 0.1$. Curves are defined as in Figure 2.

the shear viscosity ratio for $k = \frac{7}{8}$ exhibits only shear thinning whereas both η/η_0 and $(\eta_E/\eta_{E0})_2$ essentially exhibit only shear thinning for $k = 1.5$. A second difference involves the ordering of the viscosity ratios for sufficiently high deformation rates for $k = \frac{7}{8}$. For dimensionless deformation rates near unity, the ordering of the viscosity ratios for $k = \frac{7}{8}$ is as follows:

$$\left(\frac{\eta_E}{\eta_{E0}}\right)_2 > \left(\frac{\eta_E}{\eta_{E0}}\right)_1 > \frac{\eta_U}{\eta_{U0}} > \frac{\eta_B}{\eta_{B0}} > \frac{\eta}{\eta_0} \quad (52)$$

If this ordering is compared with the result for $k = 1.5$ [eq. (25)], it is evident that the major difference is that the viscosity ratio $(\eta_E/\eta_{E0})_2$ is greatest for $k = \frac{7}{8}$ and least for $k = 1.5$. It is not known whether the ordering in eq. (52) is valid for a polystyrene solution with $k = \frac{7}{8}$ since the necessary data do not exist. It is, of course, possible that this predicted ordering is an incorrect prediction of strain-coupling theory. With the exception of the position of $(\eta_E/\eta_{E0})_2$, the ordering presented in eq. (52) is reasonable. In addition, as noted above, the ordering in eq. (25) represents both experimental data and the prediction of strain-coupling theory for $k = 1.5$.

This study was supported by funds provided by the Dow Chemical Co.

REFERENCES

1. J. S. Vrentas, D. C. Venerus, and C. M. Vrentas, *J. Polym. Sci. Polym. Phys. Ed.,* **29,** 537 (1991).
2. J. S. Vrentas, C. M. Vrentas, and D. C. Venerus, *J. Non-Newtonian Fluid Mech.,* **42,** 351 (1992).
3. J. S. Vrentas, C. M. Vrentas, and D. C. Venerus, *Rheol. Acta,* **32,** 74 (1993).
4. J. S. Vrentas and C. M. Vrentas, *J. Appl. Polym. Sci.,* **49,** 733 (1993).
5. J. S. Vrentas, C. M. Vrentas, and D. C. Venerus, *Macromolecules,* **23,** 5133 (1990).
6. J. S. Vrentas, D. C. Venerus, and C. M. Vrentas, *Rheol. Acta,* **29,** 298 (1990).
7. J. S. Vrentas and C. M. Vrentas, *Rheol. Acta,* **34,** 109 (1995).
8. J. S. Vrentas, D. C. Venerus, and C. M. Vrentas, *J. Non-Newtonian Fluid Mech.,* **40,** 1 (1991).
9. J. S. Vrentas and C. M. Vrentas, *Rheol. Acta,* **34,** 281 (1995).
10. H. M. Laun and H. Schuch, *J. Rheol.,* **33,** 119 (1989).